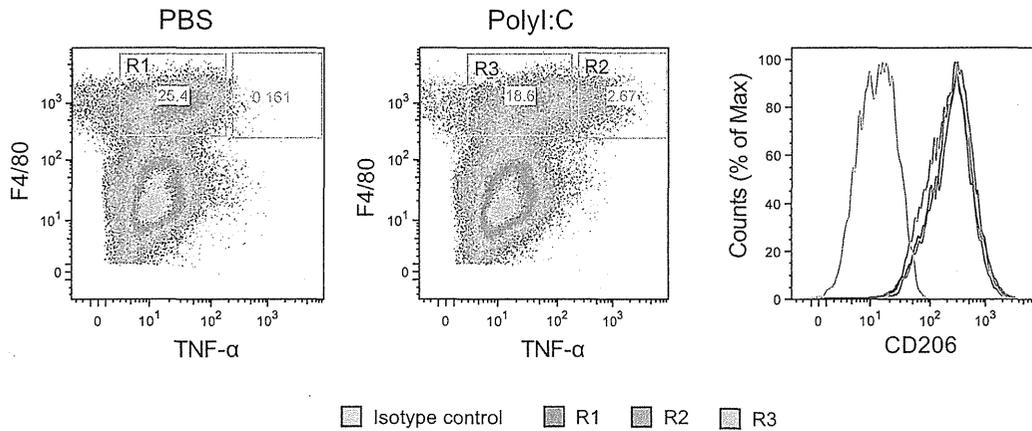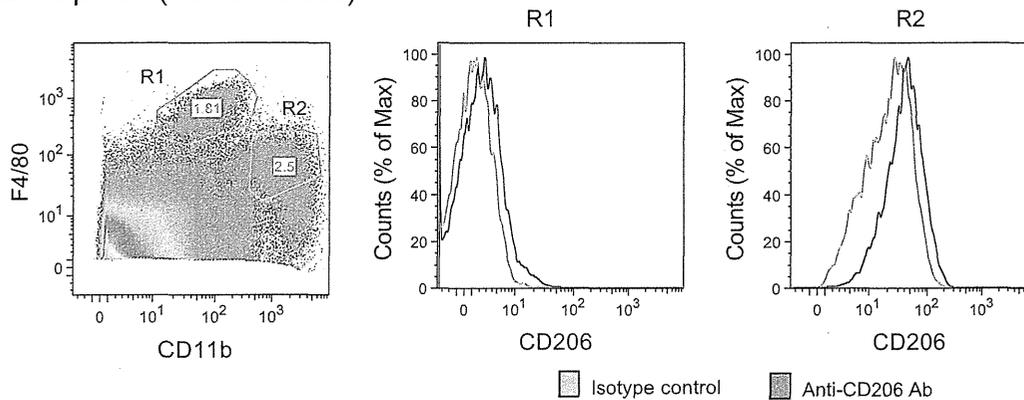## A 3LL tumor

B Spleen (naive mouse)

Fig. S6. Both TNF-α–producing and –nonproducing F4/80⁺ macrophages in 3LL tumor of polyI:C-injected mouse express CD206 (macrophage mannose receptor). (*A*) 3LL tumor-bearing mice were injected i.p with 200 μg polyI:C. After 1 h, single-cell suspension of tumor was incubated in the presence of 10 μg/mL Brefeldin A for 3 h. Intracellular cytokine staining for TNF-α in CD45.2⁺F4/80⁺ cells was performed. R2, and R1 and R3 indicates TNF-α–producing and –nonproducing F4/80⁺ cells, respectively. (*B*) CD206 expression in splenic F4/80⁺CD11b⁺ cells (R1 and R2) of naive mouse.
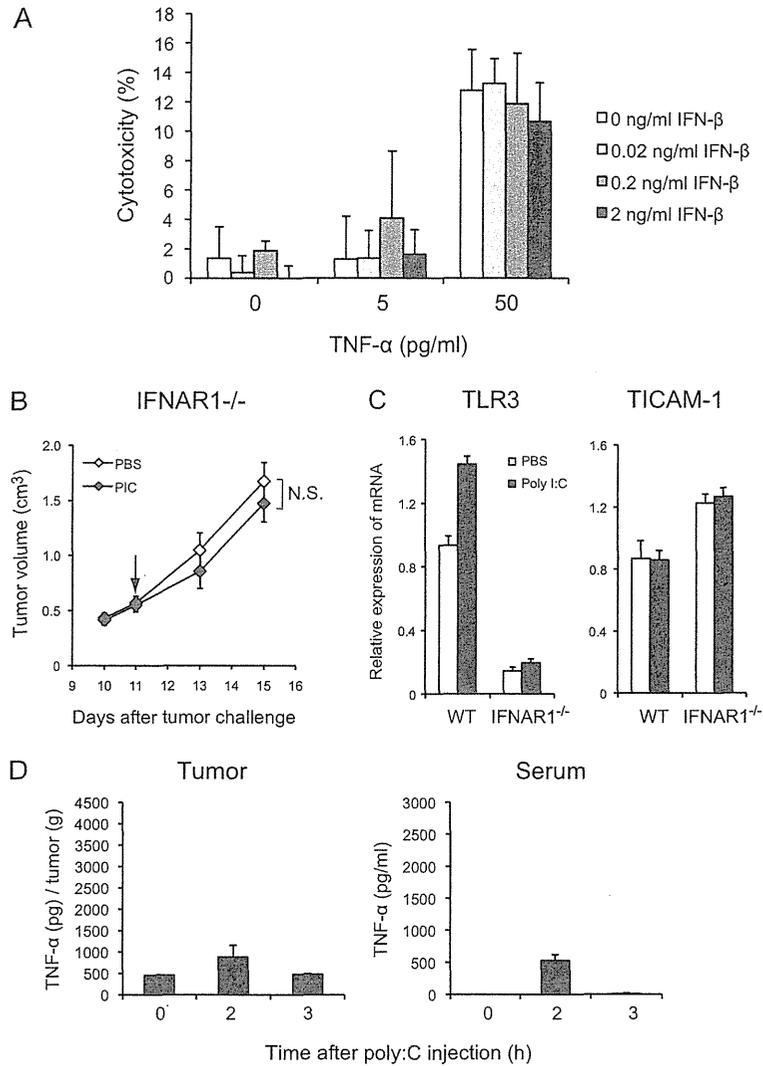
Fig. S7. Involvement of type I IFN signaling in 3LL tumor regression induced by polyI:C. (A) Effect of IFN-β on cytotoxic activity of TNF-α against 3LL tumor cells. 3LL cells were incubated in the presence of 0, 5, and 50 pg/mL recombinant mouse TNF-α in combination with 0, 0.02, 0.2, and 2 ng/mL recombinant mouse IFN-β. Cytotoxicity was determined by ^{51}Cr release assay. (B) Disabling polyI:C for 3LL tumor regression in IFN-α/β receptor (IFNAR1)$^{-/-}$ mice. PolyI:C was i.p injected on day 11; n = 3–4 mice per group. Data are shown as average ± SE. N.S., not significant. (C) Levels of the mRNA of TLR3 and TICAM-1 in 3LL tumor-associated F4/80$^+$ cells of WT or IFNAR1$^{-/-}$ mice. (D) TNF-α levels in tumor and serum in polyI:C-stimulated IFNAR$^{-/-}$ mice. Mice bearing 3LL tumors were i.p. injected with 200 μg polyI:C. Tumor (*Left*) and serum (*Right*) were collected at 0, 2, and 3 h after polyI:C injection, and TNF-α concentration was determined by ELISA. TNF-α level in tumor is presented as [TNF-α protein (pg)/tumor weight (g)].
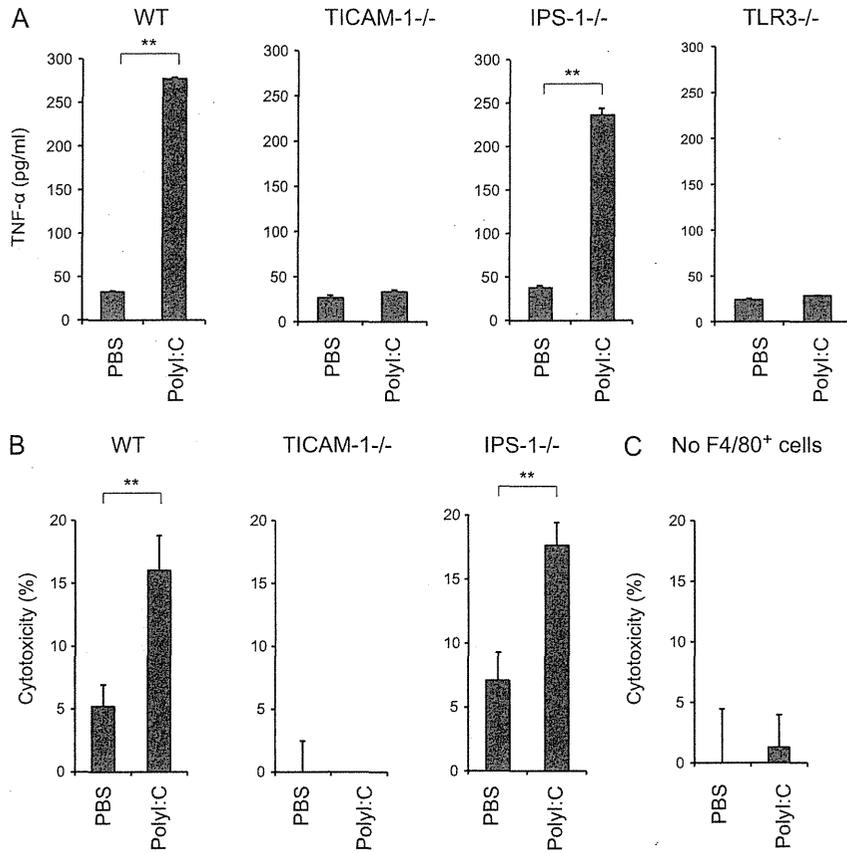
Fig. S8. In vitro polyI:C-stimulated F4/80+ cells secrete TNF-α and have cytotoxic activity. (A) F4/80+ cells isolated from 3LL tumor were stimulated with polyI:C (50 μg/mL) in vitro. After 24 h, the conditioned medium was collected and TNF-α concentration was determined by ELISA. (B) F4/80+ cells isolated from tumor were mixed with ^{51}Cr-labeled 3LL tumor cells in the presence or absence of polyI:C (50 μg/mL). After 20 h, radioactivity of the conditioned medium was measured. E/T = 10. (C) ^{51}Cr-labeled 3LL tumor cells were incubated for 20 h in the presence or absence of polyI:C (50 μg/mL); n = 3. Data are shown as average ± SD. **P < 0.001. A representative experiment of three with similar outcomes is shown.

A

IFN-β

Fold increase

16
14
12
10
8
6
4
2
0

WT   TICAM-1-/-   IPS-1-/-

IL-12p40

Fold increase

16
14
12
10
8
6
4
2
0

WT   TICAM-1-/-   IPS-1-/-

Cxcl11

Fold increase

70
60
50
40
30
20
10
0

WT   TICAM-1-/-   IPS-1-/-

IL-6

Fold increase

25
20
15
10
5
0

WT   TICAM-1-/-   IPS-1-/-

B

Arg1

Fold increase

3.0
2.5
2.0
1.5
1.0
0.5
0

WT   TICAM-1-/-   IPS-1-/-

Chi3l3

Fold increase

1.8
1.6
1.4
1.2
1.0
0.8
0.6
0.4
0.2
0

WT   TICAM-1-/-   IPS-1-/-

MMR

Fold increase

1.8
1.6
1.4
1.2
1.0
0.8
0.6
0.4
0.2
0

WT   TICAM-1-/-   IPS-1-/-

MMP9

Fold increase

1.8
1.6
1.4
1.2
1.0
0.8
0.6
0.4
0.2
0

WT   TICAM-1-/-   IPS-1-/-

VEGFA

Fold increase

1.8
1.6
1.4
1.2
1.0
0.8
0.6
0.4
0.2
0

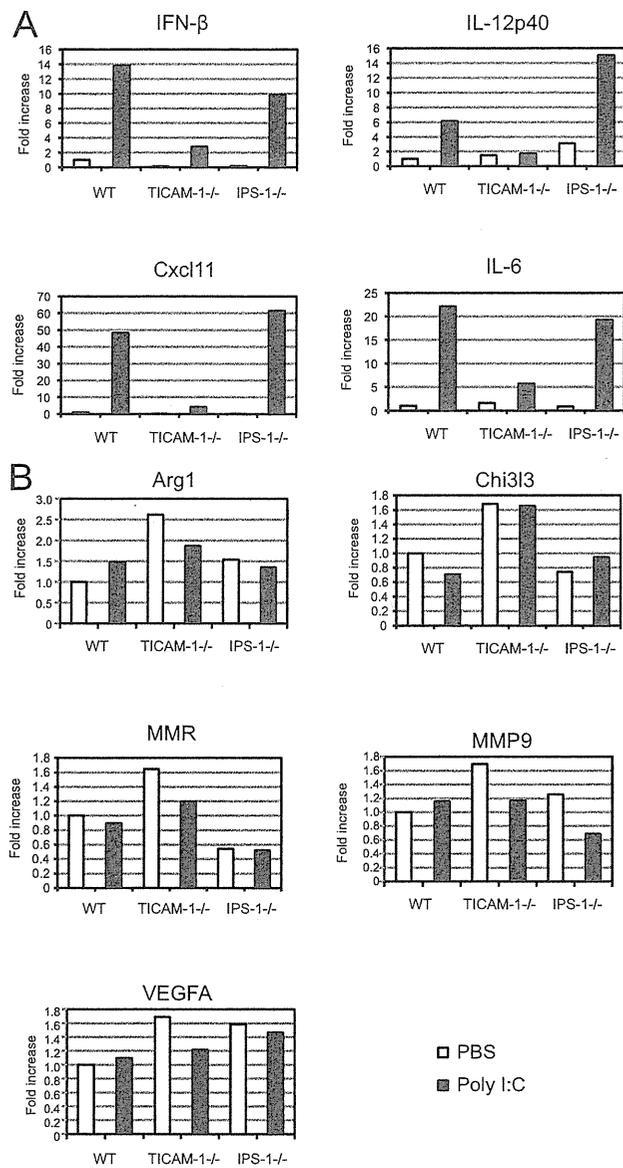WT   TICAM-1-/-   IPS-1-/-

□ PBS
▨ Poly I:C

Fig. S9. PolyI:C induces the expression of M1 but not M2 macrophage-associated genes in tumor-infiltrated F4/80⁺ cells through the TICAM-1 pathway. 3LL tumor-bearing mice were i.p injected with 200 μg polyI:C. After 3 h, tumors pooled from two mice treated with polyI:C or PBS were mixed. F4/80⁺ cells were isolated from the mixed tumor, and the expression of (A) M1- and (B) M2-related genes was analyzed. A representative experiment of two with similar outcomes is shown.
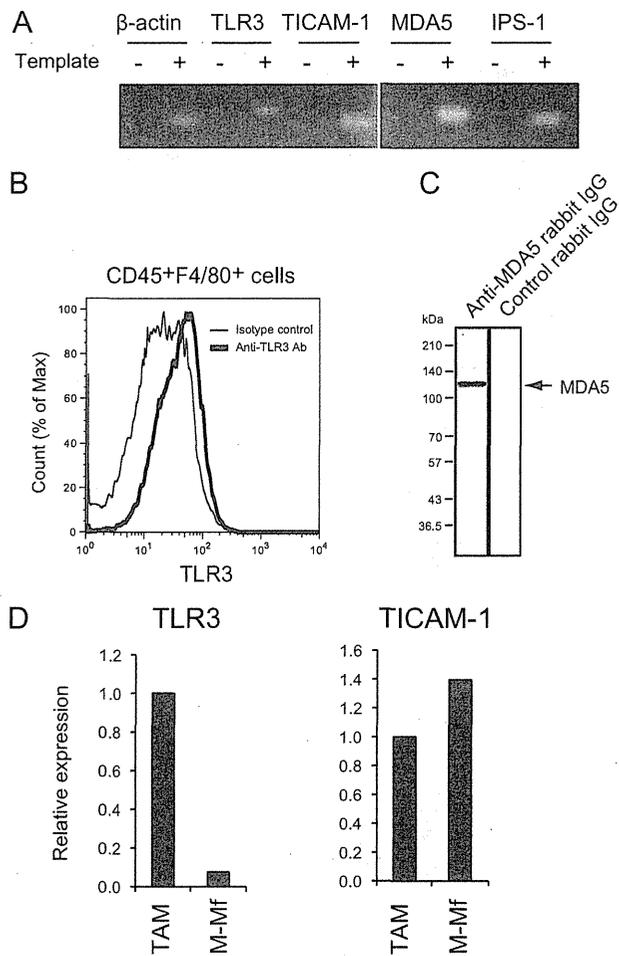
A

	β-actin		TLR3		TICAM-1		MDA5		IPS-1	
Template	-	+	-	+	-	+	-	+	-	+

B

CD45+F4/80+ cells

C

← MDA5

D

TLR3

TICAM-1

Fig. S10. Expression of TLR3 and MDA5 in 3LL tumor-associated F4/80+ cells. (A) mRNA expression of TLR3, TICAM-1, MDA5, and IPS-1 in 3LL tumor-associated F4/80+ cells. Total RNA (1 μg) of F4/80+ cells isolated from 3LL tumor was used as a template for RT-PCR analysis. (B) Single-cell suspension of 3LL tumor was stained with FITC-labeled anti-CD45 and PE-labeled anti-F4/80 antibody, followed by intracellular staining with Alexa 647-labeled anti-TLR3 antibody (11F8) or isotype control antibody (rat IgG2a). CD45+F4/80+ cells are shown. (C) Cytoplasmic extract of F4/80+ cells was subjected to SDS/PAGE and immunoblotted with rabbit anti-MDA5 antibody or control IgG purified from rabbit serum. (D) mRNA expression of TLR3 and TICAM-1 in F4/80+ tumor-associated macrophages (TAM) and macrophage colony-stimulating factor-induced bone marrow-derived macrophages (M-Mf).
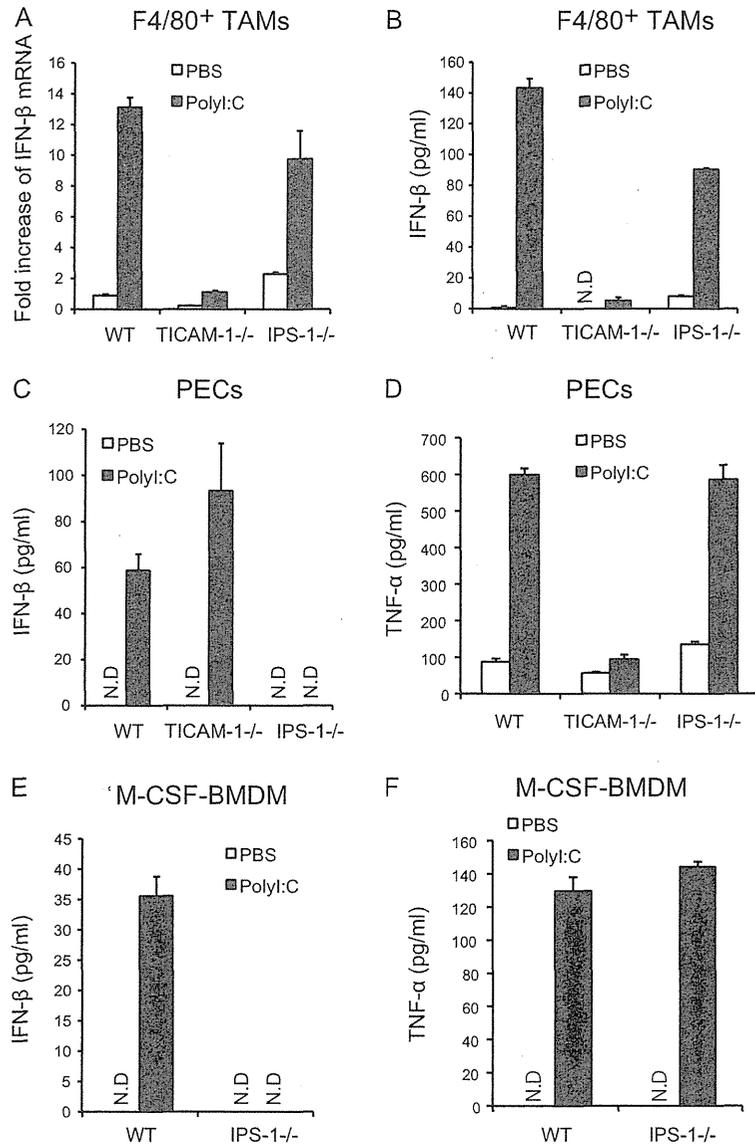
265

A F4/80⁺ TAMs

B F4/80⁺ TAMs

C PECs

D PECs

E M-CSF-BMDM

F M-CSF-BMDM

Fig. S11. In vitro stimulation with polyI:C increases the production of IFN-β and TNF-α by Mfs. (A and B) F4/80⁺ cells were isolated from 3LL tumor implanted in WT, TICAM-1⁻ᐟ⁻, and IPS-1⁻ᐟ⁻ mice and stimulated with 50 μg/mL polyI:C. After 4 h, cells were harvested and IFN-β mRNA expression was analyzed by quantitative PCR analysis (A). After 20 h, IFN-β concentration in culture supernatant was determined by ELISA (B). (C and D) Peritoneal exudate cells (PECs) isolated from WT, TICAM-1⁻ᐟ⁻, and IPS-1⁻ᐟ⁻ mouse were stimulated with 50 μg/mL polyI:C for 20 h. The concentrations of IFN-β (C) and TNF-α (D) in culture supernatant were determined by ELISA. (E and F) Macrophage colony-stimulating factor (M-CSF)-induced bone marrow-derived macrophages (BMDM) were prepared from WT and IPS-1⁻ᐟ⁻ mouse and cultured in the presence of 30% L929 supernatant containing M-CSF. After 6 d, adherent cells were harvested and stimulated with 50 μg/mL polyI:C for 20 h. The concentrations of IFN-β (E) and TNF-α (F) in culture supernatant were determined by ELISA. Data are shown as mean ± SD (n = 3). N.D., not detected. A representative experiment of two with similar outcomes is shown.

Table S1. Expression of various markers on 3LL and MC38 tumor cells

Surface marker	3LL	MC38
H2-K[b]	–	++
H2-D[b]	±	++
RAE1	++	Not determined
CD45	–	–

Expression of surface markers was analyzed by flow cytometry. Expression was evaluated by mean fluorescence shift: –, ~0.99 ; ±, 1~10 ; +, 11~100 ; ++, 101~.

Table S2. RT-PCR primers used in this study

	Forward primer (5′–3′)	Reverse primer (5′–3′)
IFN-β	CCAGCTCCAAGAAAGGACGA	CGCCCTGTAGGTGAGGTTGAT
IL-12p40	AATGTCTGCGTGCAAGCTCA	ATGCCCACTTGCTGCATGA
IL-6	GTGCATCATCGTTGTTCATACAATC	CTGGGAAATCGTGGAAATGAG
TNF-α	AGGGATGAGAAGTTCCCAAATG	GCTTGTCACTCGAATTTTGAGAAG
IL-1β	TGACGGACCCCAAAAGATGA	TGCTGCTGCGAGATTTGAAG
IL-10	GGCGCTGTCATCGATTTCTC	TGCTCCACTGCCTTGCTCTTA
Cxcl11	GGCTGCGACAAAGTTGAAGTGA	TCCTGGCACAGAGTTCTTATTGGAG
IRF4	AGCCCAGCAGGTTCATAACTACA	CCTCGTGGGCCAAACGT
IRF5	GGTCAACGGGGAAAAGAAACT	CATCCACCCCTTCAGTGTACT
Jmjd3	CGAGTGGTTCGCGGTACAT	GAAGCGGTAAACAGGAATATTGGA
Arg1	GGAATCTGCATGGGCAACCTGTGT	AGGGTCTACGTCTCGCAAGCCA
MMP9	CAAGTGGGACCATCATAACATCA	GATCATGTCTCGCGGCAAGT
VEGFA	GACATCTTCCAGGAGTACC	TGCTGTAGGAAGCTCATCT
Chi3l3	TCACTTACACACATGAGCAAGAC	CGGTTCTGAGGAGTAGAGACCA
Mrc1	CTCTGTTCAGCTATTGGACGC	CGGAATTTCTGGGATTCAGCTTC
Retnla	CCAATCCAGCTAACTATCCCTCC	ACCCAGTAGCAGTCATCCCA
GAPDH	GCCTGGAGAAACCTGCCA	CCCTCAGATGCCTGCTTCA

Table S3. Expression of surface markers on tumor-infiltrated F4/80⁺ cells

Marker	Expression*
I-Ab	+
H2-D^b	+
H2-K^b	+
CD80	++
CD86	++
CD40	±
CD11c	±
CD3	−
CD4	−
CD8α	−
Gr1	+
B220	+
CD11b	+++
CD206 (MMR)	++

*Expression was evaluated by mean fluorescence shift: −, ~0.99 ; ±, 1 ~10 ; +, 11 ~100 ; ++, 101 ~1,000 ; +++, 1,001~.

267

Dendritic Cells from Oral Cavity Induce Foxp3⁺ Regulatory T Cells upon Antigen Stimulation

Sayuri Yamazaki[1,2]*[9], Akira Maruyama[1][9], Kohei Okada[1], Misako Matsumoto[1], Akimichi Morita[2], Tsukasa Seya[1]*

1 Department of Microbiology and Immunology, Graduate School of Medicine, Hokkaido University, Sapporo, Japan, 2 Department of Geriatric and Environmental Dermatology, Nagoya City University, Graduate School of Medical Sciences, Nagoya, Japan

Abstract

Evidence is accumulating that dendritic cells (DCs) from the intestines have the capacity to induce Foxp3⁺CD4⁺ regulatory T cells (T-regs) and regulate immunity versus tolerance in the intestines. However, the contribution of DCs to controlling immunity versus tolerance in the oral cavity has not been addressed. Here, we report that DCs from the oral cavity induce Foxp3⁺ T-regs as well as DCs from intestine. We found that oral-cavity-draining cervical lymph nodes contained higher frequencies of Foxp3⁺ T-regs and ROR-γt⁺ CD4⁺T cells than other lymph nodes. The high frequency of Foxp3⁺ T-regs in the oral-cavity-draining cervical lymph nodes was not dependent on the Toll like receptor (TLR) adaptor molecules, Myd88 and TICAM-1 (TRIF). In contrast, the high frequency of ROR-γt⁺ CD4⁺T cells relies on Myd88 and TICAM-1. In vitro data showed that CD11c⁺ DCs from oral-cavity-draining cervical lymph nodes have the capacity to induce Foxp3⁺ T-regs in the presence of antigen. These data suggest that, as well as in the intestinal environment, antigen-presenting DCs may play a vital role in maintaining tolerance by inducing Foxp3⁺ T-regs in the oral cavity.

Introduction

Foxp3⁺CD25⁺CD4⁺ regulatory T cells (T-regs), constitute about 5–10% of peripheral CD4⁺T cells and control immunological self-tolerance in rodents and human [1,2,3,4]. The expansion and induction of CD25⁺Foxp3⁺ T-regs in the periphery are controlled by professional antigen-presenting cells, dendritic cells (DCs) [5,6]. DCs can expand thymic-derived natural occurring T-regs [7,8,9]. DCs are the most efficient antigen presenting cells to induce Foxp3⁺T-regs from Foxp3⁻ precursors in the periphery [10,11]. Peripheral DCs directly control the numbers and homeostasis of Foxp3⁺T-regs in vivo [12].

Foxp3⁺T-regs induced by DCs in the intestine control the balance between inflammation and tolerance in the gut [13,14,15]. CD103⁺DCs in the intestine use the retinoic acid-metabolizing enzyme retinaldehyde dehydrogenase and induce Foxp3⁺T-regs to maintain oral tolerance [16,17]. Intestinal DCs use signaling through ß-catenin to induce Foxp3⁺T-regs, which suppress Th17 and Th1 responses in the intestine [18]. Specific pathogens or Toll-like receptor (TLR) signals have been shown to induce Foxp3⁺T-regs in the intestine [19,20]. Moreover, Foxp3⁺T-regs control Th17 cells using interleukin (IL)-10 in the intestine [21,22]. Thus, Foxp3⁺T-regs in the intestine are important in maintaining mucosal tolerance where there are vast numbers of commensal microbes and food antigens.

As in the intestine, many commensal microbes and food antigens also exist in the oral cavity [23,24,25,26]. Oral cavity is often involved with systemic immunological diseases such as graft versus host diseases, Stevens-Johnson syndrome, Behçet diseases, pemphigus vulgaris and Sjögren's syndrome. In addition, oral cavity is the place where many viruses, including influenza, herpes, common cold etc., start to infect. Therefore, it is important to identify how immune response is regulated in the oral cavity. Here we found that the DCs from oral cavity have the capacity to induce Foxp3⁺T-regs. To our knowledge, this is the first report showing that DCs from the oral cavity induce Foxp3⁺T-regs to maintain tolerance.

Results

The Frequency of Foxp3⁺T-regs is Increased in Cervical Lymph Nodes (CLNs) in a Myd88/TICAM-1- Independent Manner

We considered whether Foxp3⁺T-regs played an important role in the skin or oral cavity because the skin and oral cavity are exposed to many commensal microbes and antigens, like the intestine. First, we investigated the frequencies of Foxp3⁺T-regs in lymph nodes (LNs) at different anatomical locations, which included skin- and oral-cavity-draining LNs. We found that

cervical LNs (CLNs) contained a higher frequency of Foxp3⁺ T-regs than other skin-draining LNs, such as axillary LNs (ALNs) and inguinal LNs (ILNs; paired t-test: p<0.005; Fig.1A arrow, Fig.1B and Fig.S1). CLNs contained a slightly, but significantly, higher frequency of Foxp3⁺ T-regs than mesenteric LNs (MLNs; paired t-test p<0.05; Fig.1B). In MLNs, Foxp3⁺T-regs are actively induced by CD103⁺ DCs [16,17]. These data suggest that Foxp3⁺T-regs may be also induced in CLNs, as in MLNs.

To investigate if the frequency of DCs correlates with the frequency of Foxp3⁺T-regs, the frequency of CD11c⁺DCs in total cells was compared between CLNs and ALNs (Fig.S2). The frequency of DCs was similar between CLNs and ALNs.

Recent reports showed that signals though TLR-2 induce Foxp3⁺T-regs [20,27,28]. To examine whether signals from TLRs are required for the high frequency of Foxp3⁺ T-regs in CLNs, we took advantage of Myd88 and TICAM-1 (TRIF) double knockout mice (Myd88/TICAM1 DKO), which lack all TLR signaling [29,30]. In Myd88/TICAM1 DKO mice, CLNs still contained a significantly higher frequency of Foxp3⁺T-regs than inguinal LNs (ILNs; paired t-test: p<0.05; Fig.1B). The frequency of Foxp3⁺T-regs in CLNs did not differ between Myd88/TICAM1 DKO and wild-type (WT) mice (t-test: p = 0.09; Fig.1B, 1C). The frequency of Foxp3⁺T-regs in MLNs did not differ between Myd88/TICAM1 DKO and WT mice also (t-test: p = 0.4; Fig.1B).

Thus, Foxp3⁺T-regs are increased in CLNs in a Myd88/TICAM1-independent manner, suggesting that TLR signals are not involved in the increase in Foxp3⁺ T-regs in CLNs.

The Frequency of ROR-γt⁺ CD4⁺T Cells is Increased in CLNs in a Myd88/TICAM1- Dependent Manner

The induction of Foxp3⁺T-regs in the intestine is reciprocally controlled by Th17 [18,31]. To examine the balance between Th17 and Foxp3⁺T-regs, we next compared the frequencies of ROR-γt⁺ CD4⁺T cells in different anatomical locations. ROR-γt is a transcription factor expressed by Th17 cells [32]. We found that CLNs had a significantly higher frequency of ROR-γt⁺ CD4⁺T cells than other skin-draining LNs and spleen (paired t-test: p<0.05; Fig.2A closed arrows and Fig.2B). As expected, MLNs contained a higher frequency of ROR-γt⁺ CD4⁺T cells than other LNs (Fig.2A gray arrows and Fig.2B).

To assess whether signals from microbes through TLRs are required for the induction of ROR-γt⁺ CD4⁺T cells in CLNs, we investigated Myd88/TICAM1 DKO mice. In Myd88/TICAM1 DKO mice, frequencies of ROR-γt⁺ CD4⁺T cells did not differ between CLNs and ILNs (paired t-test: p = 0.05; Fig.2B). Moreover, the frequency of ROR-γt⁺ CD4⁺T cells in CLNs was significantly reduced in Myd88/TICAM-1 DKO mice (t-test: p<0.05; Fig.2B). The frequency of ROR-γt⁺ CD4⁺T cells in MLNs did not differ between Myd88/TICAM1 DKO and WT mice also (t-test: p = 0.1; Fig.2B).

Thus, both Foxp3⁺T-regs and Th17 may be induced in CLNs. However, Myd88/TICAM1 signaling is important for the development of ROR-γt⁺CD4⁺-Th17 T cells in CLNs (Fig.2B), but not for the induction of Foxp3⁺T-regs (Fig.1B).

CLNs are Oral-cavity-draining Lymph Nodes

We considered that the higher frequency of Foxp3⁺T-regs in CLNs may reflect their response to antigens in the oral cavity. To confirm whether CLNs were draining LNs from the oral cavity, we investigated the proliferation of transferred OT-II CD4⁺-T cells in CLNs after sublingual (s.l.) administration of ovalbumin (OVA; Fig.3). OT-II mice are commonly used OVA-specific CD4⁺ T-cell receptor transgenic mice [7,10,28]. In the absence of OVA s.l.

administration, carboxyfluorescein diacetate succinimidyl ester (CFSE)-labeled OT-II T cells did not divide, in CLNs or ALNs (Fig.3, top). With OVA s.l. administration, CFSE-labeled OT II T cells divided well in CLNs (Fig.3, bottom arrow), but not in ALNs. Thus, we confirmed that CLNs were draining LNs of the oral cavity because s.l.-administered OVA antigen was presented to OT II CD4⁺-T cells.

DCs from Oral-cavity-draining CLNs Locate Close to Foxp3⁺T-regs and have the Capacity to Induce Foxp3⁺ T-regs on Antigen Stimulation

Next, to investigate the interaction between DCs and Foxp3⁺T-regs in CLNs, we microscopically examined CLNs. We found that Foxp3⁺T-regs and CD11c⁺ DCs were closely located, as reported previously in MLNs [33] (Fig.4A). This suggests that DCs from CLNs may induce Foxp3⁺T-regs as DCs do in MLNs.

To determine whether DCs from the oral cavity can in fact induce Foxp3⁺T-regs, we compared the capacity to induce Foxp3⁺T-regs in vitro using DCs from ALNs, MLNs, and oral-cavity-draining CLNs. Purified CD11c⁺ DCs from CLNs, ALNs, or MLNs were cultured with OT II CD4⁺T cells with or without antigen for 5 days. In the presence of antigen, CLN DCs induced a higher frequency of Foxp3⁺T-regs compared with ALN DCs (paired t-test: p<0.005; Fig.4B, 4C). The frequency of Foxp3⁺T-regs induced by antigen plus DCs did not differ between the culture with CLN DCs and that with MLN DCs (paired t-test: p = 0.878; Fig.4C).

These results indicated that DCs from the oral-cavity-draining CLNs had the capacity to induce Foxp3⁺T-regs with antigen, as DCs from MLNs do.

CD103⁺DCs may not be Involved in Inducing Foxp3⁺ T-regs in Oral-cavity-draining CLNs

To determine whether DCs from the oral cavity contain a specific DC subset to induce Foxp3⁺T-regs as in the intestine, we first performed real-time PCR. When we investigated the mRNA expression of retinal dehydrogenase 2 (RALDH2), transforming growth factor (TGF)-ß, and IL-10, there was no difference between DCs from CLNs and ALNs (Fig.4A). DCs from MLNs had higher mRNA expression of RALDH2 as previously reported (Fig.5A). We also measured the protein production of TGF-ß1 and IL-10 in the culture supernatant. TGF-ß1 was not detected in the culture supernatants of CLN DCs with or without latent TGF-ß activation (data not shown). We did not detect IL-10 in the culture supernatants from CLN DCs and OT II CD4⁺T cells without peptide in Fig.4B and 4C (data not shown). Theses results indicate that TGF-ß1, IL-10 and RALDH2 may not involve in the induction of Foxp3⁺T-regs by CLN DCs.

To investigate whether CD103⁺DCs play a role in inducing Foxp3⁺T-regs in CLNs, we compared the frequency of CD103⁺DCs in each location. However, oral cavity-draining CLNs had a lower frequency of CD103⁺ DCs than MLNs (Fig.5B).

Plasmacytoid DCs have a capacity to induce Foxp3⁺T-regs [34,35,36,37]. Epidermal Langerhans cells and migratory dermal DCs have also been reported to induce Foxp3⁺T-regs [38,39,40]. However, the frequencies of plasmacytoid DCs and migratory class II^high DCs did not differ between CLNs and ALNs (Fig.5C). Next, we investigated the classical CD8⁺ and CD8⁻ DC subsets in CLNs and ALNs. The frequency of CD8⁺ DCs was similar between CLNs and ALNs (paired t test: p = 0.065) (Fig.5D). However, CLNs had a significantly higher frequency of CD8⁻ DCs than ALNs (paired t test: p<0.0005) (Fig.5D).
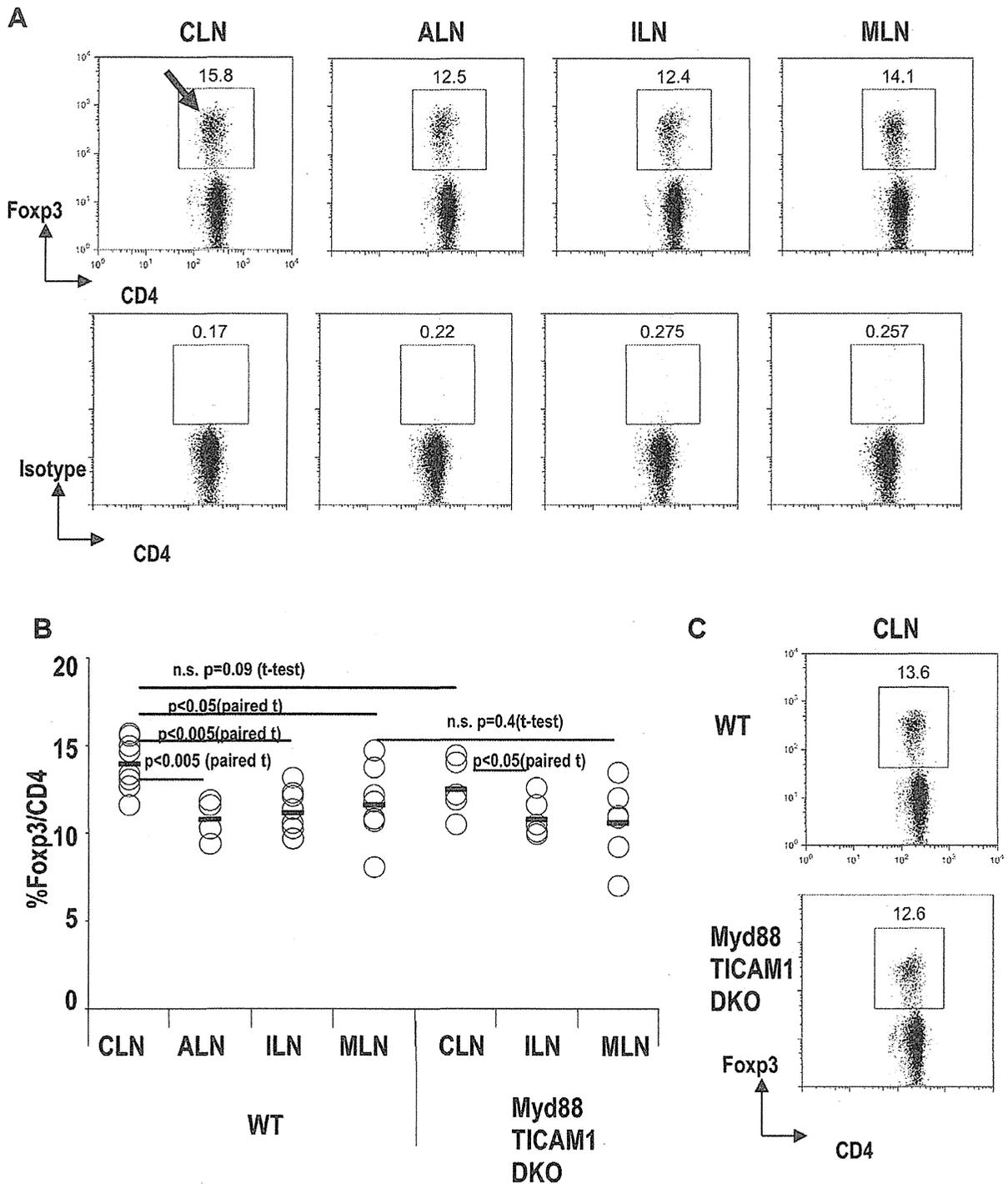
Figure 1. Frequency of Foxp3+ T-regs in cervical lymph node is increased in a Myd88/TICAM-1 independent manner. (A) Cervical lymph nodes (CLN), axillary lymph nodes (ALN), inguinal lymph nodes (ILN), and mesenteric lymph nodes (MLN) from wild type B6 mice were analyzed for the expression of Foxp3. The isotype control is shown at the bottom. Plots were gated on CD4+ T cells. Representative of seven separate experiments. (B) As in (A), but CLN, ALN, ILN and MLN from wild-type B6 mice (WT) or Myd88/TICAM1 double knockout mice (Myd88/TICAM1 DKO) were analyzed for the expression of Foxp3. Summary from seven separate experiments. P value provided is by paired t-test or t-test. "n.s."="not significant". (C) As in (B), but a representative of CLN is shown.
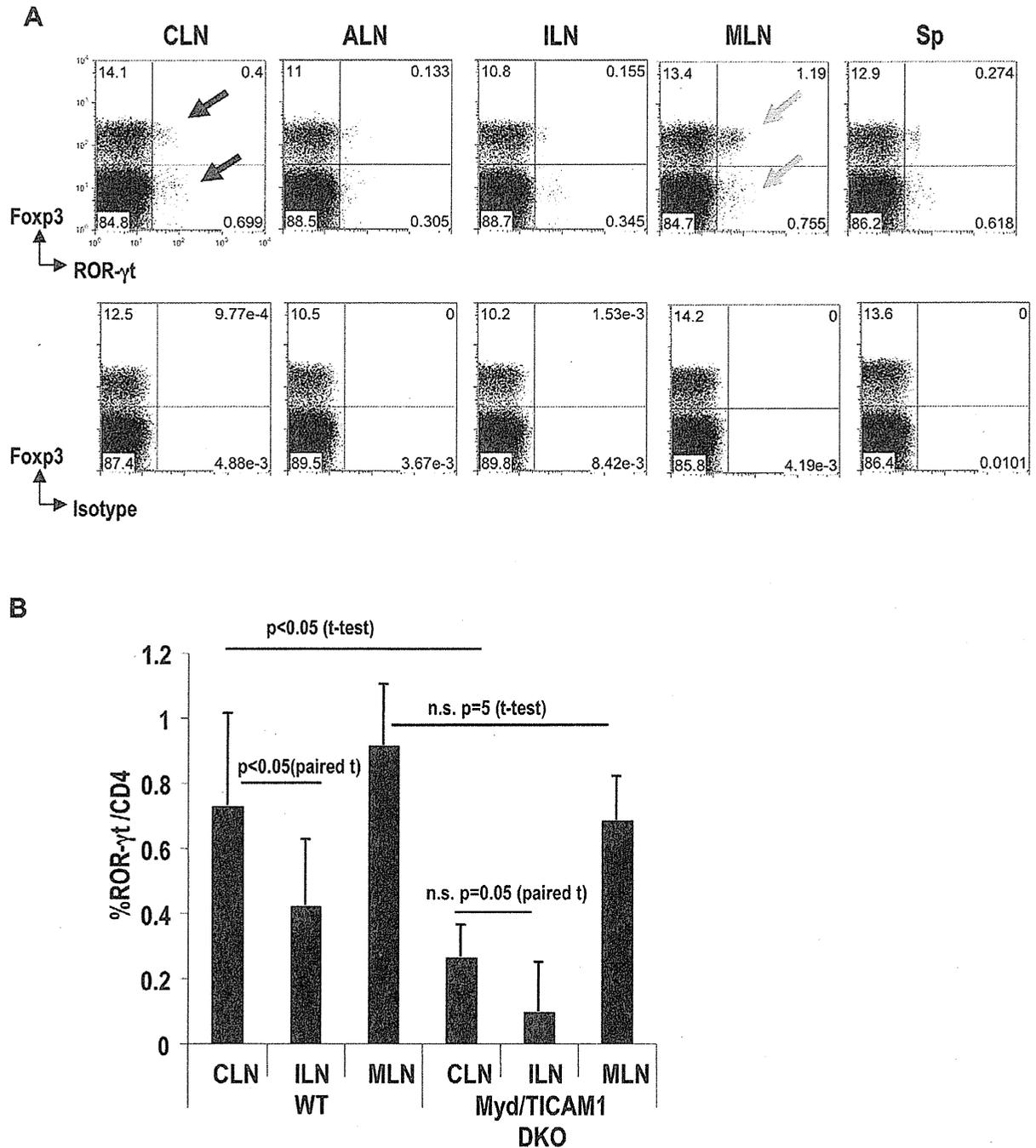doi:10.1371/journal.pone.0051665.g001

A

B

Figure 2. Frequency of ROR-γt⁺CD4⁺ T cell in cervical lymph node is increased in a Myd88/TICAM-1 dependent manner. (A) CLN, ALN, ILN, MLN, and spleen (Sp) from WT B6 mice were analyzed for the expression of Foxp3 and ROR-γt. The plots were gated on CD4⁺ T cells. Isotype staining for ROR-γt is shown at the bottom. Representative of three separate experiments. (B) As in (A), but cells from WT mice or Myd88/TICAM-1 DKO mice were analyzed for the expression of ROR-γt and CD4. The graphic shows a summary from two separate experiments. P value provided is by paired-t test or t-test. "n.s." = "not significant".
doi:10.1371/journal.pone.0051665.g002

These results suggest that CD103⁺ DCs and retinoic acid may not contribute to inducing Foxp3⁺T-regs in CLNs. It is possible that the classical CD8⁻ DC subset in CLNs may participate in the induction of Foxp3⁺T-regs. Further studies are required.
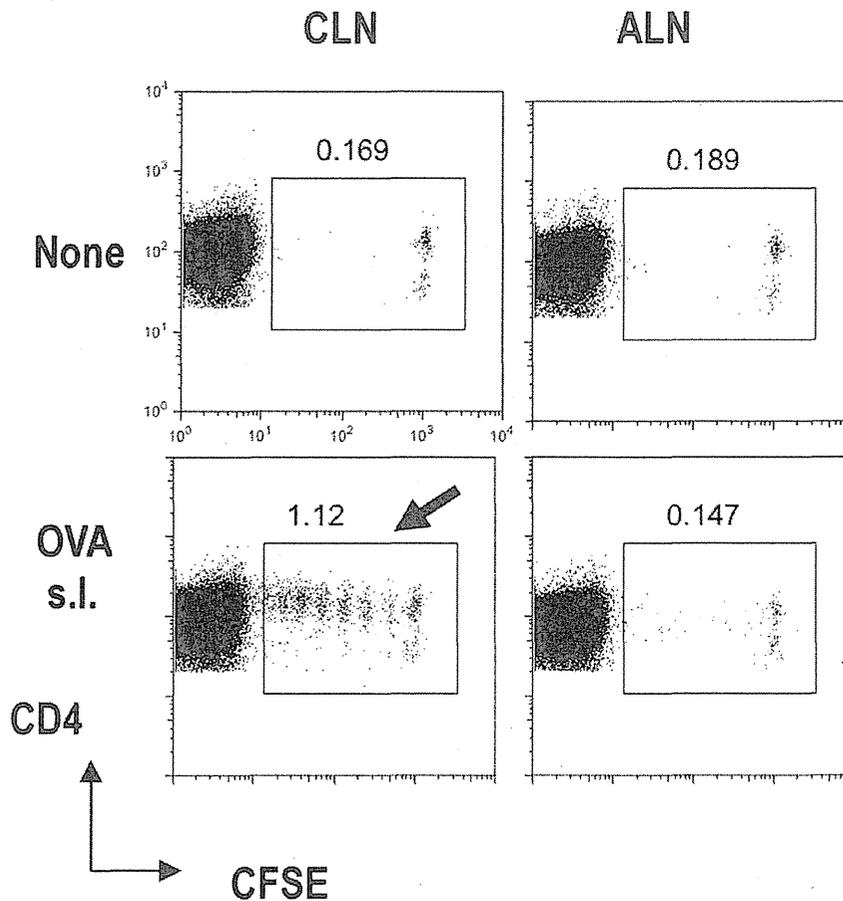
271

CLN   ALN

None

0.169   0.189

OVA
s.l.

1.12   0.147

CD4

CFSE

Figure 3. Cervical lymph nodes are draining lymph nodes from the oral cavity. CFSE-labeled OTII CD4+T cells were adoptively transferred into B6 mice on day −1. On day 0, 500 μg of OVA was administered sublingually (s.l.). CLN or ALN was analyzed for CFSE dilution at day 3. One of two similar experiments is shown for the FACS plots. Plots were gated on CD4+T cells.
doi:10.1371/journal.pone.0051665.g003

Discussion

The oral cavity is exposed to many antigens and commensal organisms every day [23,24,25,26]. The oral cavity is frequently associated with systemic immunological disorders, such as graft versus host diseases, Stevens-Johnson syndrome and Behçet diseases. However, it is unknown how tolerance in the oral cavity is maintained. Here, we showed that the balance between Th17 and Foxp3+T-regs may play a role in maintaining tolerance in the oral cavity. We found that the frequencies of Foxp3+T-regs and ROR-γt +CD4+T cells were increased in oral-cavity-draining CLNs, compared with skin-draining LNs and mesenteric LNs. DCs from oral-cavity-draining CLNs have the capacity to induce Foxp3+ T-regs in vitro on antigen stimulation, as much as DCs from mesenteric LNs do. These data suggest that the induced Foxp3+T-regs in oral-cavity-draining CLNs may be important in maintaining mucosal tolerance in response to microbes and food antigens in the oral cavity.

Although some TLR signaling is involved in inducing Foxp3+ T-regs [20,27,28,41,42], the high frequency of Foxp3+ T-regs in CLNs was not dependent on Myd88/TICAM1 (Fig. 1). Thus, TLR signaling is apparently not involved in the induction of Foxp3+T-regs in the oral cavity. However, we cannot exclude the possibility that some specific microbes may be involved in the inducing Foxp3+T-regs in the oral cavity in a Myd88/TICAM1 independent manner. For example, Atarashi et al recently showed that Clostridum induces Foxp3+T-regs in the colon in a Myd88-independent manner [19]. It might be interesting to investigate if there are specific microbes that contribute to the induction of Foxp3+T-regs in the oral cavity, especially as the bacterial community varies between the oral cavity and gut [26].

Our results showed that the high frequency of ROR-γt+CD4+T cells was dependent on Myd88/TICAM1 in the oral-cavity-draining CLNs (Fig.2). This is consistent with recent findings in skin [43]. Th17 cells in skin are reduced in Myd88/TICAM1 knockout mice and skin-resident commensal bacteria induce Th17 cells in a Myd88- and IL-1 receptor-dependent manner [43]. It is also known that some microbes induce Th17 using TLR signals; for example, Th17 cells induced by Chlamydia infection are reduced in Myd88 KO mice [44]. Thus, it is possible that TLR signals through some oral microbes are responsible for the increase of ROR-γt +CD4+T cells in oral-cavity-draining CLNs. Interestingly, the intestine may use a different mechanism from the oral cavity and skin to maintain Th17 cells, because Th17 cells are not reduced in the intestine in Myd88/TICAM1(TRIF)-knock out mice [45,46].
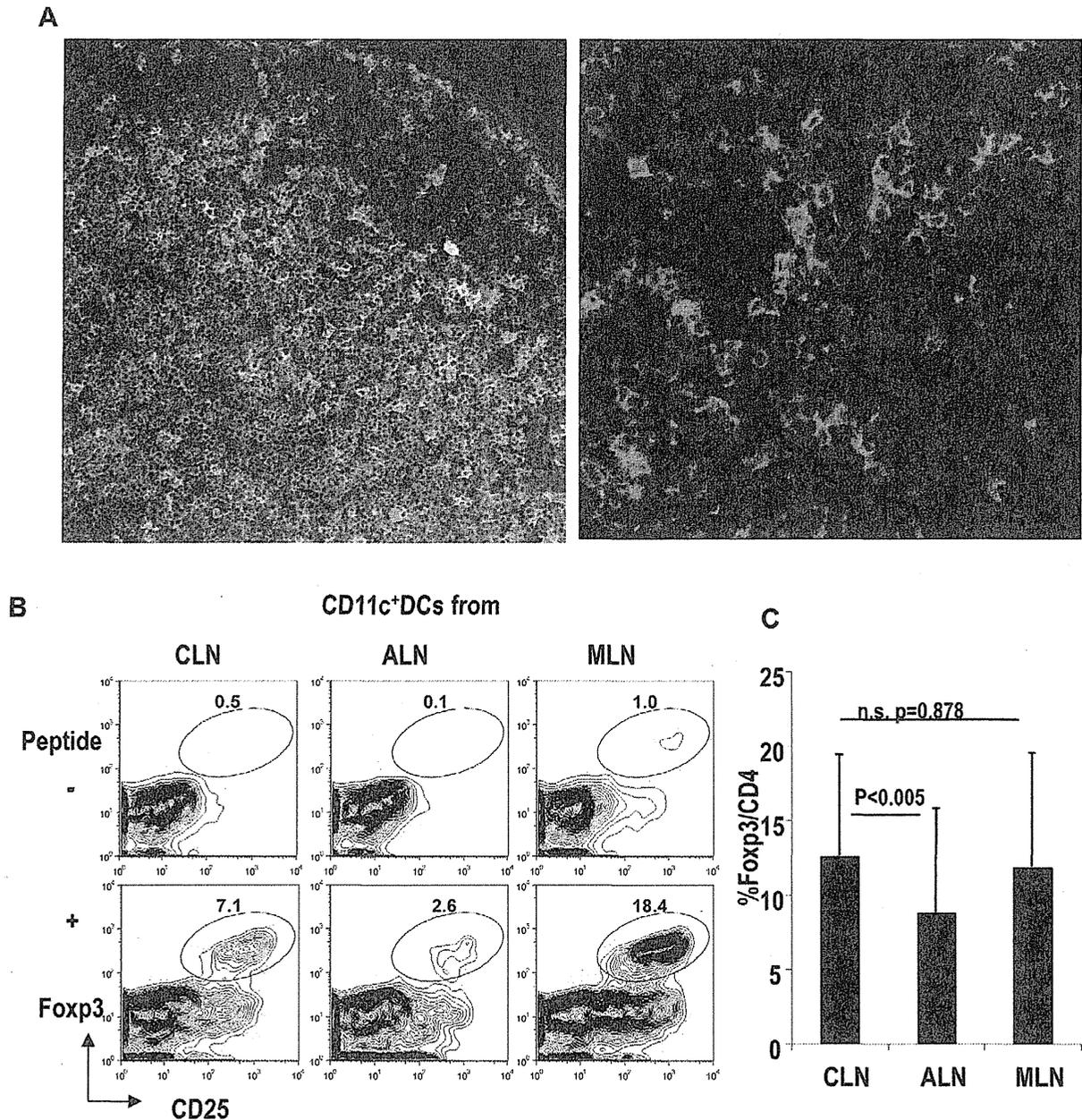
272

Figure 4. Dendritic cells from oral-cavity-draining cervical lymph nodes induce Foxp3⁺ T-regs. (A) CLNs were stained with Foxp3 (red), CD4 (green) and CD11c (blue). Representative of three similar separate experiments. (B) OT II CD4⁺ T cells (5×10⁴) were cultured with dendritic cells (DCs) from CLN, ALN, or MLN (5×10⁴) with or without OVA peptide. After 5 days, cells were stained with Foxp3, CD25 and CD4. The plots were gated on CD4⁺ T cells. Representative of four separate experiments. (C) As in (A), but the graphic shows a summary of four separate experiments. P value provided is by paired t-test. "n.s." = "not significant".
doi:10.1371/journal.pone.0051665.g004

Furthermore, we found that DCs from oral-cavity-draining CLNs induce Foxp3⁺T-regs in the presence of antigen, as do DCs from MLNs (Fig.4B). It has been reported that cutaneous CD103⁺DCs induce Foxp3⁺T-regs using RALDH2, as intestinal CD103⁺DCs do [47]. Here, we would like to propose that DCs in the oral cavity use a different mechanism(s) to induce Foxp3⁺Tregs from DCs in the intestine. First, CLNs have few CD103⁺ DCs

compared with MLNs (Fig. 5B). Second, DCs from CLNs do not express RALDH2 at the mRNA level (Fig. 5A). We have not yet found any specific DC subset in the oral-cavity-draining CLNs. However, CD8⁻ classical DCs are increased in CLNs versus ALNs. Our previous report showed that CD8⁺DEC205⁺DCs induce Foxp3⁺T-regs from Foxp3⁻ cells and that CD8⁻33D1⁺DCs expand natural occurring Foxp3⁺T-regs
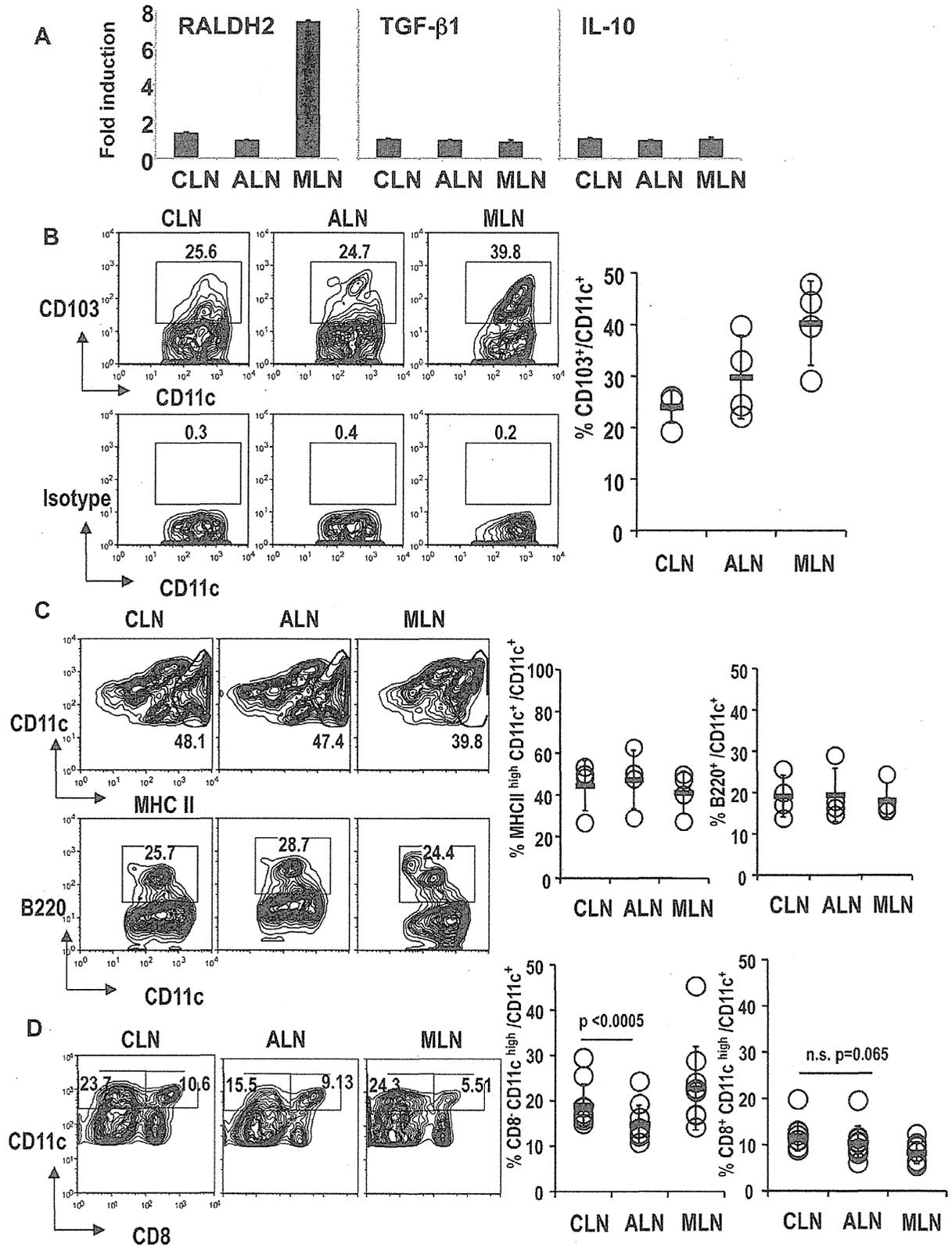
274

[6,11]. Thus, it seems possible that CD8⁻DCs in CLNs may participate in expanding natural occurring Foxp3⁺T-regs.

Recently, it has been reported that recently activated Foxp3⁺T-regs from CLNs accumulated in CLNs after adoptive transfer [48]. It was suggested that TCR-mediated signals upon antigen stimulation may play a key role in the site-specific accumulation of Foxp3⁺T-regs in CLNs. Taken together, oral-cavity-draining CLNs may be a special location where Foxp3⁺T-regs are induced and also accumulate.

Here we showed that Foxp3⁺T-regs are induced in oral-cavity-draining CLNs in a Myd88/TICAM1 independent manner and that DCs from oral-cavity-draining CLNs have the capacity to induce Foxp3⁺Tregs on antigen stimulation. The mechanisms by which DCs to induce Foxp3⁺T-regs may differ from those in the intestine. We propose that Foxp3⁺T-regs play an important role in maintaining tolerance in the oral cavity to suppress Th17, as in the intestine. DCs from CLNs play a key role in maintaining tolerance upon oral antigen stimulation in the oral cavity. Further studies are required to identify the mechanism(s) by which DCs to induce Foxp3⁺T-regs in the oral cavity.

Materials and Methods

Mice

C57BL6J (B6) mice were from Japan Clea (Tokyo). Myd88 KO mice were from Dr. Shizuo Akira (Osaka University). TICAM-1 KO mice were established in our laboratory [29,30]. OT-II OVA CD4 T cell receptor transgenic mice were kindly provided by Dr. Kazuya Iwabuchi (Kitasato University). The mice were maintained in the Hokkaido University Animal Facility in a specific pathogen-free condition. All experiments used mice between 6-12-week-old mice at the time of first procedure. All mice were used according to the guidelines of the institutional animal care and use committee of the Hokkaido University, who approved this study (ID number: 08-0243, "Analysis of immune modulation by toll-like receptors.").

Antibodies and Reagents

PE-conjugated CD103, CD25 (PC61), Alexa-488 conjugated anti-CD25 (7D4), FITC, biotin or APC conjugated CD4 (RM4-5), CD11c, B220, NK1.1, purified anti-CD16/CD32 (2.4G2) antibodies were from Biolegend (San Diego, CA). Anti-CD11c, and streptavidin microbeads were from Miltenyi Biotec (Gladbach, Germany). CFSE was from Molecular Probes (Eugene, OR). PE conjugated anti-mouse ROR-γt antibody and the anti-mouse Foxp3 (FJK-16s) staining kit were from eBioscience (San Diego, CA). LPS free OVA protein was from Seikagaku Co.(Tokyo, Japan).

Cell Isolation

CD4⁺ T cells were first negatively separated by MACS beads from lymph nodes and spleen cell suspensions (>90%; Miltenyi Biotech). CD4⁺ T cells were sometimes further purified by FACS Aria II (BD Bioscience, Franklin Lakes, NJ). CD11c⁺ DCs from spleen, CLNs, ALNs, or MLNs were selected with anti-CD11c beads (Miltenyi Biotech) [7,10].

Co-culture with T cells and DCs

CD4⁺T cells from OT II transgenic mice were cultured with DCs at 0 or 0.01-μM OVA peptide for 5 days. After 5 days, each culture was stained with Foxp3, following the manufacturer's protocol. Cells were acquired by FACS calibur flow cytometer (BD). Analyses were performed using the Flowjo software (TreeStar, USA).

Adoptive Transfer of OT-II CD4⁺T cells

CD4⁺T cells from OT II transgenic mice were labeled with 5 μM CFSE, and 1×10⁶ T cells were injected intravenously into B6 recipients. One day later, OVA protein was administered sublingually. After 3 days, mice were sacrificed, and CLNs and ALNs were stained with CD4 and CFSE dilution was investigated. Cells were assessed by FACS calibur (BD). Analyses were performed using the Flowjo software (TreeStar, USA).

Quantitative PCR

Total RNA was isolated with TRIzol (Invitrogen), and reversed-transcribed with the High Capacity cDNA Transcription Kit (ABI) according to manufacturer's instructions. qPCR was performed with the Step One Real-Time PCR system (ABI). All primers for real-time PCR have been reported previously [27,28].

Measuring Cytokine Production

The purified DCs (1×10⁵) were cultured in serum free RPMI medium for 20 h. The concentrations of TGF-ß in the supernatants were measured by TGF-ßELISA kit (R&D). Following the manufacturer's instructions, we measured the TGF-ß with or without activation of the latent form of TGF-ß. Culture supernatants with OT II CD4⁺T cells and DCs were measured for IL-10 by ELISA (eBiosciences) or Cytometric Bead Array (BD Bioscience). Analysis with the Cytometric Bead Array was performed according to the manufacturer's instructions.

Confocal Microscopy

CLNs were sectioned, fixed with acetone, and stained with anti-CD4-FITC and CD11c-APC antibodies. After permeabilization with the buffer from the Foxp3 staining kit (eBioscience), they were stained with an anti-Foxp3-PE antibody. They were washed and observed by confocal microscopy (LSM510 META, Zeiss, Jena, Germany).

Supporting Information

Figure S1 CD25⁺ and CD25⁻ Foxp3⁺ T-regs in lymph nodes and spleen. (A) CLN, ALN, ILN, MLN and Sp from B6 mice were analyzed for the expression of Foxp3 and CD25. The isotype control for Foxp3 is shown at the bottom. Plots were gated on CD4⁺ T cells. Representative of 2 separate experiments is

shown. (B) As in (A), but the frequency of CD25+ or CD25−
Foxp3+ T-regs/CD4+T cells were shown.
(TIF)

**Figure S2 The frequency of CD11c+ DC is similar
between CLN and ALN.** (A) CLN or ALN from one B6 mouse
were digested by collagenase and stained with anti-CD11c and
CD8 Abs. Representative of 5 separate experiments is shown. (B)
The frequency of CD11c+ cells/total LN cells in one mouse is
shown. A summary of 5 separate experiments. P value provided is
by paired t-test. "n.s." = "not significant".
(TIF)

Author Contributions

Conceived and designed the experiments: SY. Performed the experiments:
A. Maruyama SY KO. Analyzed the data: SY A. Maruyama MM A.
Morita TS. Wrote the paper: SY.

References

1. Sakaguchi S, Yamaguchi T, Nomura T, Ono M (2008) Regulatory T cells and immune tolerance. Cell 133: 775–787.
2. Sakaguchi S, Miyara M, Costantino CM, Hafler DA (2010) FOXP3+ regulatory T cells in the human immune system. Nature reviews Immunology 10: 490–500.
3. Rudensky AY (2011) Regulatory T cells and Foxp3. Immunological reviews 241: 260–268.
4. Bour-Jordan H, Bluestone JA (2009) Regulating the regulators: costimulatory signals control the homeostasis and function of regulatory T cells. Immunological reviews 229: 41–66.
5. Yamazaki S, Inaba K, Tarbell KV, Steinman RM (2006) Dendritic cells expand antigen-specific Foxp3+ CD25+ CD4+ regulatory T cells including suppressors of alloreactivity. Immunological reviews 212: 314–329.
6. Yamazaki S, Steinman RM (2009) Dendritic cells as controllers of antigen-specific Foxp3+ regulatory T cells. Journal of dermatological science 54: 69–75.
7. Yamazaki S, Iyoda T, Tarbell K, Olson K, Velinzon K, et al. (2003) Direct expansion of functional CD25+ CD4+ regulatory T cells by antigen-processing dendritic cells. The Journal of experimental medicine 198: 235–247.
8. Fehervari Z, Sakaguchi S (2004) Control of Foxp3+ CD25+CD4+ regulatory cell activation and function by dendritic cells. International immunology 16: 1769–1780.
9. Yamazaki S, Patel M, Harper A, Bonito A, Fukuyama H, et al. (2006) Effective expansion of alloantigen-specific Foxp3+ CD25+ CD4+ regulatory T cells by dendritic cells during the mixed leukocyte reaction. Proceedings of the National Academy of Sciences of the United States of America 103: 2758–2763.
10. Yamazaki S, Bonito AJ, Spisek R, Dhodapkar M, Inaba K, et al. (2007) Dendritic cells are specialized accessory cells along with TGF-ß for the differentiation of Foxp3+ CD4+ regulatory T cells from peripheral Foxp3 precursors. Blood 110: 4293–4302.
11. Yamazaki S, Dudziak D, Heidkamp GF, Fiorese C, Bonito AJ, et al. (2008) CD8+ CD205+ splenic dendritic cells are specialized to induce Foxp3+ regulatory T cells. Journal of immunology 181: 6923–6933.
12. Darrasse-Jeze G, Deroubaix S, Mouquet H, Victora GD, Eisenreich T, et al. (2009) Feedback control of regulatory T cell homeostasis by dendritic cells in vivo. The Journal of experimental medicine 206: 1853–1862.
13. Izcue A, Coombes JL, Powrie F (2009) Regulatory lymphocytes and intestinal inflammation. Annual review of immunology 27: 313–338.
14. Barnes MJ, Powrie F (2009) Regulatory T cells reinforce intestinal homeostasis. Immunity 31: 401–411.
15. Hand T, Belkaid Y (2010) Microbial control of regulatory and effector T cell responses in the gut. Current opinion in immunology 22: 63–72.
16. Coombes JL, Siddiqui KR, Arancibia-Carcamo CV, Hall J, Sun CM, et al. (2007) A functionally specialized population of mucosal CD103+ DCs induces Foxp3+ regulatory T cells via a TGF-beta and retinoic acid-dependent mechanism. The Journal of experimental medicine 204: 1757–1764.
17. Sun CM, Hall JA, Blank RB, Bouladoux N, Oukka M, et al. (2007) Small intestine lamina propria dendritic cells promote de novo generation of Foxp3 T reg cells via retinoic acid. The Journal of experimental medicine 204: 1775–1785.
18. Manicassamy S, Reizis B, Ravindran R, Nakaya H, Salazar-Gonzalez RM, et al. (2010) Activation of beta-catenin in dendritic cells regulates immunity versus tolerance in the intestine. Science 329: 849–853.
19. Atarashi K, Tanoue T, Shima T, Imaoka A, Kuwahara T, et al. (2011) Induction of colonic regulatory T cells by indigenous Clostridium species. Science 331: 337–341.
20. Round JL, Lee SM, Li J, Tran G, Jabri B, et al. (2011) The Toll-like receptor 2 pathway establishes colonization by a commensal of the human microbiota. Science 332: 974–977.
21. Huber S, Gagliani N, Esplugues E, O'Connor W Jr, Huber FJ, et al. (2011) Th17 cells express interleukin-10 receptor and are controlled by Foxp3- and Foxp3+ regulatory CD4+ T cells in an interleukin-10-dependent manner. Immunity 34: 554–565.
22. Chaudhry A, Samstein RM, Treuting P, Liang Y, Pils MC, et al. (2011) Interleukin-10 signaling in regulatory T cells is required for suppression of Th17 cell-mediated inflammation. Immunity 34: 566–578.
23. Avila M, Ojcius DM, Yilmaz O (2009) The oral microbiota: living with a permanent guest. DNA and cell biology 28: 405–411.
24. Sansonetti PJ (2011) To be or not to be a pathogen: that is the mucosally relevant question. Mucosal immunology 4: 8–14.
25. Grice EA, Kong HH, Conlan S, Deming CB, Davis J, et al. (2009) Topographical and temporal diversity of the human skin microbiome. Science 324: 1190–1192.
26. Costello EK, Lauber CL, Hamady M, Fierer N, Gordon JI, et al. (2009) Bacterial community variation in human body habitats across space and time. Science 326: 1694–1697.
27. Manicassamy S, Ravindran R, Deng J, Oluoch H, Denning TL, et al. (2009) Toll-like receptor 2-dependent induction of vitamin A-metabolizing enzymes in dendritic cells promotes T regulatory responses and inhibits autoimmunity. Nature medicine 15: 401–409.
28. Yamazaki S, Okada K, Maruyama A, Matsumoto M, Yagita H, et al. (2011) TLR2-dependent induction of IL-10 and Foxp3+CD25+CD4+ regulatory T cells prevents effective anti-tumor immunity induced by Pam2 lipopeptides in vivo. PloS One 6: e18833.
29. Oshiumi H, Matsumoto M, Funami K, Akazawa T, Seya T (2003) TICAM-1, an adaptor molecule that participates in Toll-like receptor 3-mediated interferon-beta induction. Nature immunology 4: 161–167.
30. Akazawa T, Ebihara T, Okuno M, Okuda Y, Shingai M, et al. (2007) Antitumor NK activation induced by the Toll-like receptor 3-TICAM-1 (TRIF) pathway in myeloid dendritic cells. Proceedings of the National Academy of Sciences of the United States of America 104: 252–257.
31. Mucida D, Park Y, Kim G, Turovskaya O, Scott I, et al. (2007) Reciprocal TH17 and regulatory T cell differentiation mediated by retinoic acid. Science 317: 256–260.
32. Ivanov, II, McKenzie BS, Zhou L, Tadokoro CE, Lepelley A, et al. (2006) The orphan nuclear receptor RORgammat directs the differentiation program of proinflammatory IL-17+ T helper cells. Cell 126: 1121–1133.
33. Onodera T, Jang MH, Guo Z, Yamasaki M, Hirata T, et al. (2009) Constitutive expression of IDO by dendritic cells of mesenteric lymph nodes: functional involvement of the CTLA-4/B7 and CCL22/CCR4 interactions. Journal of immunology 183: 5608–5614.
34. Ochando JC, Homma C, Yang Y, Hidalgo A, Garin A, et al. (2006) Alloantigen-presenting plasmacytoid dendritic cells mediate tolerance to vascularized grafts. Nature immunology 7: 652–662.
35. Hanabuchi S, Ito T, Park WR, Watanabe N, Shaw JL, et al. (2010) Thymic stromal lymphopoietin-activated plasmacytoid dendritic cells induce the generation of FOXP3+ regulatory T cells in human thymus. Journal of immunology 184: 2999–3007.
36. Chen W, Liang X, Peterson AJ, Munn DH, Blazar BR (2008) The indoleamine 2,3-dioxygenase pathway is essential for human plasmacytoid dendritic cell-induced adaptive T regulatory cell generation. Journal of immunology 181: 5396–5404.
37. Seneschal J, Clark RA, Gehad A, Baecher-Allan CM, Kupper TS (2012) Human epidermal Langerhans cells maintain immune homeostasis in skin by activating skin resident regulatory T cells. Immunity 36: 873–884.
38. Azukizawa H, Dohler A, Kanazawa N, Nayak A, Lipp M, et al. (2011) Steady state migratory RelB+ langerin+ dermal dendritic cells mediate peripheral induction of antigen-specific CD4+ CD25+ Foxp3+ regulatory T cells. European journal of immunology 41: 1420–1434.
39. Kautz-Neu K, Noordegraaf M, Dinges S, Bennett CL, John D, et al. (2011) Langerhans cells are negative regulators of the anti-Leishmania response. The Journal of experimental medicine 208: 885–891.
40. Gomez de Aguero M, Vocanson M, Hacini-Rachinel F, Taillardet M, Sparwasser T, et al. (2012) Langerhans cells protect from allergic contact dermatitis in mice by tolerizing CD8+ T cells and activating Foxp3+ regulatory T cells. The Journal of clinical investigation 122: 1700–1711.
41. Sutmuller RP, den Brok MH, Kramer M, Bennink EJ, Toonen LW, et al. (2006) Toll-like receptor 2 controls expansion and function of regulatory T cells. The Journal of clinical investigation 116: 485–494.
42. Round JL, Mazmanian SK (2010) Inducible Foxp3+ regulatory T-cell development by a commensal bacterium of the intestinal microbiota. Proceedings of the National Academy of Sciences of the United States of America 107: 12204–12209.

276

43. Naik S, Bouladoux N, Wilhelm C, Molloy MJ, Salcedo R, et al. (2012) Compartmentalized Control of Skin Immunity by Resident Commensals. Science.
44. Zhang X, Gao L, Lei L, Zhong Y, Dube P, et al. (2009) A MyD88-dependent early IL-17 production protects mice against airway infection with the obligate intracellular pathogen Chlamydia muridarum. Journal of immunology 183: 1291–1300.
45. Atarashi K, Nishimura J, Shima T, Umesaki Y, Yamamoto M, et al. (2008) ATP drives lamina propria T(H)17 cell differentiation. Nature 455: 808–812.
46. Ivanov, II, Atarashi K, Manel N, Brodie EL, Shima T, et al. (2009) Induction of intestinal Th17 cells by segmented filamentous bacteria. Cell 139: 485–498.
47. Guilliams M, Crozat K, Henri S, Tamoutounour S, Grenot P, et al. (2010) Skin-draining lymph nodes contain dermis-derived CD103- dendritic cells that constitutively produce retinoic acid and induce Foxp3+ regulatory T cells. Blood 115: 1958–1968.
48. Lieberman SM, Kim JS, Corbo-Rodgers E, Kambayashi T, Maltzman JS, et al. (2012) Site-specific accumulation of recently activated CD4+ Foxp3+ regulatory T cells following adoptive transfer. European journal of immunology 42: 1429–1435.

REVIEW

In vitro models for analysis of the hepatitis C virus life cycle

Hussein H. Aly[1,2], Kunitada Shimotohno[3], Makoto Hijikata[4] and Tsukasa Seya[1]

[1]Department of Microbiology and Immunology, Hokkaido University Graduate School of Medicine, Kita-15, Nishi-7, Kita-ku, [2]Laboratory of Viral Hepatitis and Host Defense, Hokkaido University Creative Research Institution, Kita-22, Nishi-7, Kita-ku, Sapporo 060-8638, [3]Research Institute, Chiba Institute of Technology, Narashino 275-0016, Chiba and [4]Department of Virology, Virus Research Institute, Kyoto University, Kyoto 606-8507, Japan

ABSTRACT

Chronic hepatitis C virus (HCV) infection affects approximately 170 million people worldwide. HCV infection is a major global health problem as it can be complicated with liver cirrhosis and hepatocellular carcinoma. So far, there is no vaccine available and the non-specific, interferon (IFN)-based treatments now in use have significant side-effects and are frequently ineffective, as only approximately 50% of treated patients with genotypes 1 and 4 demonstrate HCV clearance. The lack of suitable *in vitro* and *in vivo* models for the analysis of HCV infection has hampered elucidation of the HCV life cycle and the development of both protective and therapeutic strategies against HCV infection. The present review focuses on the progress made towards the establishment of such models.

Key words hepatitis C virus, HuH-7 cell, knockout mice, type I interferon.

Chronic HCV infection is a major cause of mortality and morbidity throughout the world, infecting approximately 3.1% of the world's population (1). Only a fraction of acutely infected individuals are able to clear the infection spontaneously, whereas approximately 80% of infected individuals develop a chronic infection (2, 3). Patients with chronic HCV are at increased risk for developing liver fibrosis, cirrhosis, and/or hepatocellular carcinoma. Currently, these long-term complications of chronic HCV infection are the leading indication for liver transplantation (4, 5). Because of the high incidence of new infections by blood transfusions in the 1980s before the discovery of the virus, and because morbidity associated with chronic HCV infection generally takes decades to develop, it is expected that the burden of disease in the near future will rise dramatically.

HCV is an enveloped flavivirus, with a positive-stranded RNA genome of approximately 9600 nucleotides. The coding region is flanked by 5′ and 3′ non-coding regions, which are important for the initiation of translation and regulation of genomic duplication, respectively. The coding region itself is composed of a single open reading frame, which encodes a polyprotein precursor of approximately 3000 amino acids. This polyprotein is cleaved by host and viral proteases into structural and NS proteins (Fig. 1). Replication of the HCV genome involves the synthesis of a full-length negative-stranded RNA intermediate, which in turn provides a template for the de novo production of positive-stranded RNA. Both these synthesis steps are mediated by the viral RNA-dependent RNA polymerase NS5B (6–8). NS5B lacks proofreading abilities, and this leads to a high mutation rate and the
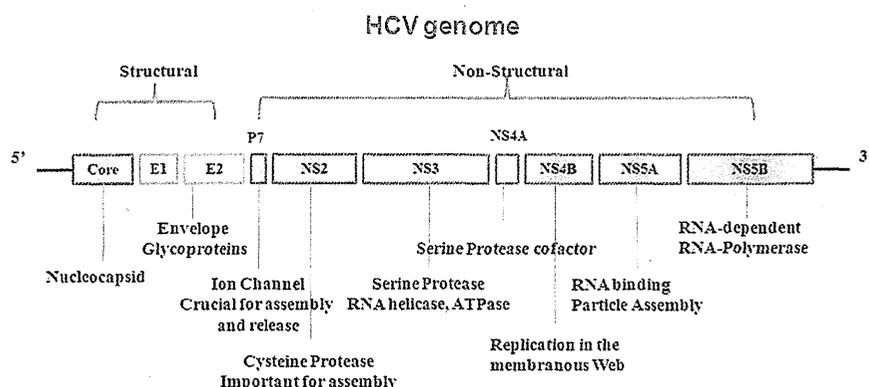
1

HCV genome

Fig. 1. Genomic structure of HCV. Genomic organization of wild-type HCV. The HCV-RNA genome consists of a major open reading frame, encoding a single polyprotein, and an alternative reading frame encoding F-proteins with unknown functions. The cleavage of the polyprotein by viral and host cell proteases gives rise to the mature structural (core, envelope proteins E1 and E2, and p7) and NS viral proteins (NS2 through NS5B). The putative activities and functions of viral proteins are indicated. The IRES located in the 5' non-coding region initiates ribosome binding and translation. Both the 5' and 3' non-coding regions are essential for viral RNA replication involving the RNA-dependent RNA polymerase NS5B. NTPase, nucleotide triphosphatase.

generation of numerous quasispecies. HCV isolates can be classified into seven major genotypes, which vary in sequence by more than 30%. In addition to the distinct prevalence and global spread of the virus, the genotype is an important factor determining disease progression and responses to antiviral therapy (9).

Currently, the only licensed treatment for HCV is the combination of (pegylated)-interferon-alpha (IFN-α) and ribavirin. Although the success rate of treatment has improved substantially, standard therapy is not effective in all patients. Moreover, severe adverse effects and high costs limit the compliance and global application of this treatment. The development of prophylaxis and novel therapeutics to treat HCV infection has been hampered by the lack of suitable *in vitro* and *in vivo* culture systems. In this review, we describe the development of *in vitro* culture systems for HCV.

Tissue culture-adapted HCV (sub-)genomic replicons

Dr Bartenschlager's group was the first to establish a convenient reproducible *in vitro* cell culture system for the study of HCV replication (10). They created antibiotic-resistant HCV genomes to select replication-competent viral clones by conveying antibiotic resistance to cells. This was achieved by replacing the structural protein-coding sequences, as well as p7 of the consensus genome Con1, by the neomycin resistance gene. In addition, a second IRES was introduced to promote translation of the non-structural protein-coding sequences important for viral replication (Fig. 2). Upon transfection of these so-called subgenomic replicons in specific cell lines, drug-resistant cell colonies were isolated in which high levels

of viral replication occurred. Subsequent analysis confirmed that these HCV replicons indeed were capable of self-amplification through synthesis of a negative-strand replication intermediate, and could be stably propagated in cell culture for many years (10, 11).

HCV replication was supported by several cell types such as HuH6 (12), HepG2 (13), Li23 (14), and 293 cells (15), with the human hepatoma cell line HuH-7 being the most permissive (16). Interestingly, removal of replicon RNA from these cell clones by treatment with type 1 IFN rendered the cells more permissive to reintroduction of replicons, resulting in higher replication rates. Examples of these highly permissive cells are HuH-7.5 and HuH-7-Lunet cells (16, 17). The efficient replication in the replicon systems was found to depend on tissue-culture-adaptive mutations. Introduction of these specific mutations in the wild-type consensus sequence significantly enhanced viral replication *in vitro* (18–22). Mutational hot spots were found clustered primarily in the NS3, NS4B, and NS5A regions. The mechanisms behind the enhanced replication caused by these tissue-culture-adaptive mutations are still largely unknown, and the interesting fact that these mutations are not commonly found in patients suggests that these may have a toll on the viral fitness.

HCV replicons have proven to be extremely valuable for studies on the process of HCV replication, as well as for testing novel antiviral compounds that specifically target the protease activity of NS3 or the polymerase activity of NS5 (23).

Cell culture-derived infectious HCV

Studies using HCV replicons have provided detailed knowledge on the mechanisms of replication of HCV.
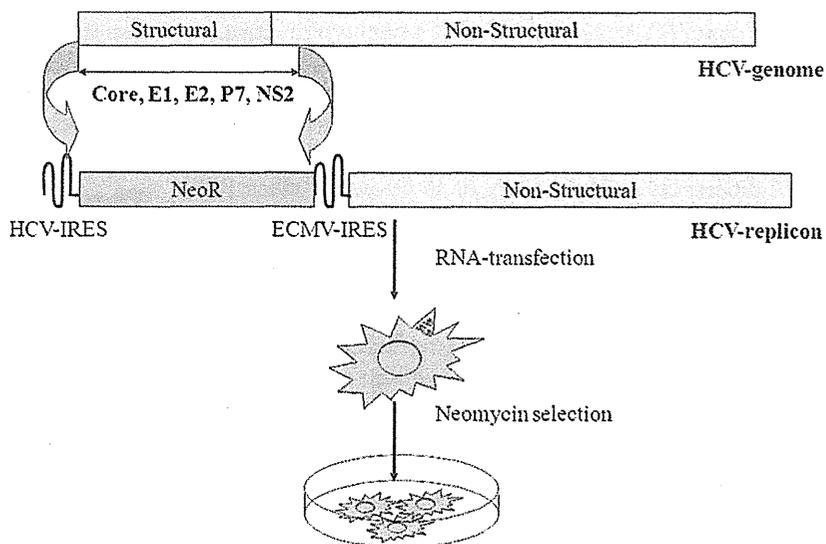
2

Fig. 2. HCV replicon system. The structural sequences (C, E1, E2, and p7) together with NS2 were replaced by a neomycin antibiotic-resistance gene, and an ECMV-IRES was introduced to drive translation of the remaining non-structural proteins. Neomycin selection of these double cistron (bicistronic) replicons in the hepatoma cell line Huh7 resulted in high-level HCV-RNA replication, depending on the gain of so-called 'tissue-culture' adaptive mutations mostly confined to the NS3, NS4B, and NS5A regions.

However, an apparent shortcoming of these models was that stable cell clones containing self-replicating replicons and expressing all viral proteins remained unable to release infectious HCV particles. The inability to secrete viral particles may be the consequence of adaptive mutations, which are needed to enhance viral replication rates, but at the same time may block viral assembly. Indeed, replicons without adaptive mutations show very low replication rates (16, 24). A different situation emerged when the first genotype 2a consensus genome was established (25, 26).

A subgenomic replicon constructed from a clone called JFH-1, isolated from a Japanese patient with fulminant hepatitis C, replicated up to 20-fold higher in HuH-7 cells as compared to Con1 replicons, and did not require adaptive mutations for efficient replication *in vitro* (26). Transfection of HuH-7 and HuH-7.5.1 cells with the

in vitro-transcribed full-length JFH-1 genome or a recombinant chimeric genome with another genotype 2a isolate, J6, resulted in the secretion of viral particles that were infectious in cultured cells (Fig. 3), in chimeric mice, and in chimpanzees (27–29).

The infectivity of cells could be neutralized with antibodies against the HCV entry receptor CD81, antibodies against E2, or immunoglobulins from chronically infected patients. Importantly, the replication of cell-cultured HCV in this system was inhibited by IFN-α as well as by several HCV-specific antiviral compounds (29). Since 2005, chimeric JFH-1-based genomes have been constructed of all seven known HCV genotypes. Similar to the J6-JFH-1 chimera, in these so-called intergenotypic recombinants, the structural genes (core, E1, and E2), p7, and NS2 of JFH-1 were replaced by genotype-specific sequences which often resulted in lower infectious virion production than
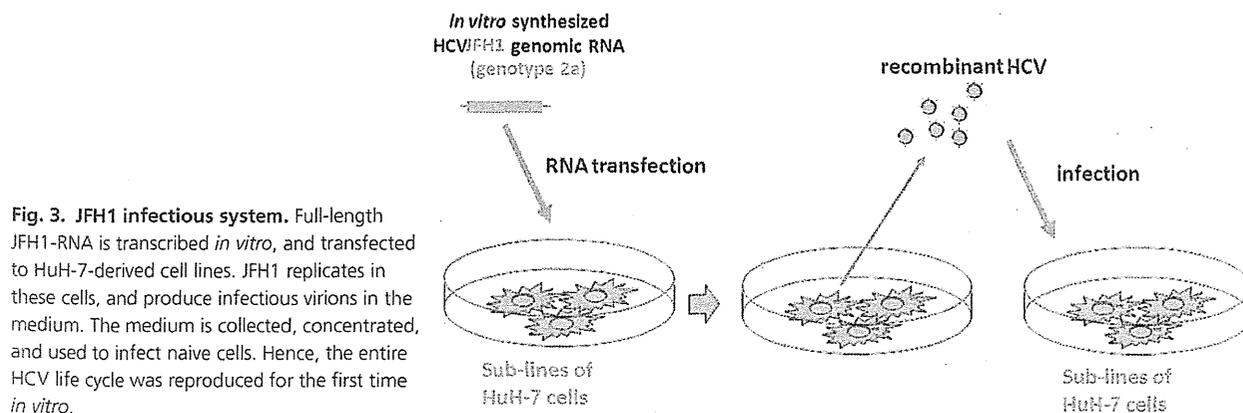

Fig. 3. JFH1 infectious system. Full-length JFH1-RNA is transcribed *in vitro*, and transfected to HuH-7-derived cell lines. JFH1 replicates in these cells, and produce infectious virions in the medium. The medium is collected, concentrated, and used to infect naive cells. Hence, the entire HCV life cycle was reproduced for the first time *in vitro*.